Hindawi
IET Electrical Systems in Transportation
Volume 2023, Article ID 6690544, 13 pages
https://doi.org/10.1049/2023/6690544

Research Article

Multiobjective Electric Vehicle Charging Network Planning Considering Chance-Constraint on the Travel Distance for Charging

Yunxiang Guo,[1] **Xinsong Zhang**,[1] **Daxiang Li**,[1] **Chenghong Gu**,[2] **Cheng Lu**,[1] **Ting Ji**,[1] **and Yue Wang**[3]

[1]*Department of Electrical Engineering, Nantong University, Nantong, China*
[2]*Department of Electronic & Electrical Engineering, University of Bath, Bath, UK*
[3]*Huaneng Nantong Power Generation Co. Ltd, Nantong, China*

Correspondence should be addressed to Xinsong Zhang; zhang.xs@ntu.edu.cn

Received 19 May 2023; Revised 2 October 2023; Accepted 31 October 2023; Published 17 November 2023

Academic Editor: I Safak Bayram

Electric vehicle charging stations (EVCSs) are important infrastructures to support sustainable development of electric vehicles (EVs), by providing convenient, rapid charging services. Therefore, the planning of electric vehicle charging network (EVCN) has attracted wide interest from both industry and academia. In this paper, a multiobjective planning model for EVCN is developed, where a fixed number of EVCSs are planned in the traffic network (TN) to achieve two objectives, i.e., minimizing both average travel distance for charging (TDfC) of EVs and investment costs of EVCN. According to the random characteristics of EVs' TDfC, its constraint is presented as a chance constraint in the developed EVCN planning model. The nondominated sorting genetic Algorithm II with the constraint domination principle (NSGA-II-CDP) is customized to solve the developed multiobjective EVCN planning model, by designing a special coding scheme, a crossover operator, and a mutation operator. Then, a maximum gradient principle of investment revenue is designed to select the optimal planning strategy from the Pareto-optimal solution set, when taking the investment return ratio as primary consideration. A 25-node TN is used to justify the effectiveness of the developed methodology.

1. Introduction

1.1. Background and Motivation. With the exacerbation of environmental pollution and the overuse of fossil fuels, electric vehicles (EVs) are receiving increasing attention in the auto market [1, 2]. Until now, rapid charging at EV charging stations (EVCSs) is one of the most commonly used charging models. The location of EVCSs can have dramatic impacts on the charging convenience for EV owners. Thus, it is critical to investigate the optimal planning strategy for EV charging networks (EVCN) in both urban areas [3] and highway networks [4, 5], to boost the shares of EVs in the auto market [6, 7].

In EVCSs, EV owners normally adopt rapid charging, whose rated power can be as high as tens or even hundreds of kW for each charger. By charging several EVs with rapid charging mode in an EVCS simultaneously, the total power could reach the level of MW, thus significantly affecting the secure and efficient operation of the power distribution system (PDS) [8–11]. Therefore, it is important to consider PDS operation in EVCN planning, so as to ensure a reliable power supply to EVCN. In detail, it requires optimizing the location and rated power for the EVCSs to mitigate adverse impacts on the PDS resulting from charging large-scale EVs [12–14].

As important service facilities in the traffic network (TN), EVCSs play a role similar to "gas stations". The primary function of EVCSs is to provide high-quality and convenient charging services to EV owners [15, 16]. Therefore, planners should pay close attention to the needs by optimizing EVCS deployments when planning the EVCN [17, 18].

Currently, EVCN is expanding at a very early stage, especially in some developing countries. It rarely exists the

scenario that multiple EVCSs are connected to the same PDS and have significant impacts on the PDS. Therefore, at this stage, the industry should take the primary function of EVCSs, i.e., providing convenient charging service to customers, as the main task in planning the EVCN. The locations of EVCSs are directly related to the convenience of charging services.

1.2. Literature Review. When planning EVCN, two types of models are mainly used to optimize the locations of EVCSs, i.e., flow-based and spatial-based models.

As to the flow-based model, Hodgson [19] developed the flow-capturing location method (FCLM) to optimize the location of the service facilities within a TN. The optimal planning strategy could maximize captured traffic flows, i.e., providing a maximal quota of service to vehicles. Kuby and Lim [20] developed the flow-refueling location model (FRLM) method by improving the FCLM, which considered available driving distances of the vehicles, thus achieving better planning strategies. Furthermore, Capar et al. [21], Kadri et al. [22], and Lee and Han [23] improved the fundamental FRLM method by considering uncertain travel distance for charging (TDfC) of EVs in calculating the traffic flow captured by the EVCN, which is therefore more practical. A generalized FRLM was introduced in [21]. This method measured the initial driving ranges of EVs as the distance between the origin and first EVCS on the EV driving paths. A multistage stochastic planning model was developed in [22] based on the generalized FRLM to derive the optimal sites of EVCSs, which was solved by the Benders decomposition approach and the genetic algorithm (GA). Lee and Han [23] developed a Benders-and-Price method to select the optimal locations for EVCSs. This method performed three advantages: (1) assuming that the distribution of maximum TDfC for EVs should be normally distributed; (2) considering uncertain characteristics of EV flows in TN, and; (3) EV owners might choose the nonshortest paths to suggested EVCSs. Convenient charging service means that EV owners could find an EVCS within their expected range when their EVs need to be charged, i.e., the shorter the average TDfC the better. This principle indicates that flow-based models [19–23] have limitations because they just devoted to maximizing the traffic flow captured by the EVCN, but have not taken the minimization of EVs' TDfC as a significant target of EVCN planning.

Different from the flow-based model, the spatial-based model was studied in [24–30] for optimizing the locations of EVCSs. Hakimi [24] developed the p-median model (PMM) to minimize the overall distance between demand and service facilities. And he improved the PMM by developing a p-median competitive location model to solve the competitive locations between different charging service providers [25]. Further, there are two other spatial-based models: the set covering model (SCM) and the maximal covering location model (MCLM). SCM is to derive the minimum number of service facilities by assuming all demands are met [26, 27]. By contrast, MCLM is to cover maximum demand under a given number of service facilities [28, 29]. PMM is compared with SCM and MCLM, based on case studies of EVCN planning in Beijing, China [30]. The results show that both SCM and MCLM ignore the distance between the demands and EVCSs, although the TDfC of EVs is believed to be significant. This, in turn, justified the fact that PMM is more effective than SCM and MCLM in solving EVCN planning problems. Nevertheless, PMM also has limitations in implementation. For example, PMM defines EV charging demand and EVCSs as nodes in TN. This would turn the dynamic process into a "node-to-node" scenario, thus neglecting charging requirement of those EVs driving in paths. Furthermore, the TDfC of EVs is highly correlated to locations of EVs in TN, thus having random characteristics. However, there is no investigation into using spatial-based model to address the random characteristics of EVs' TDfC.

1.3. Contribution and Paper Organization. In the current research, neither the flow-based model nor the spatial-based model takes EVs' TDfC, which seriously affects the charging convenience of EVs, as an important consideration when planning the EVCN. To address the limitations described above, this paper develops a novel multiobjective EVCN planning model with a chance constraint on the random TDfC of EVs. The proposed method has two objectives: (a) to minimize the average TDfC of EVs, (b) to minimize the investment in EVCN construction. The candidate sites are given beforehand as a planning boundary according to the topologies of TN and conditions of PDS. The optimization is solved by the nondominated sorting genetic Algorithm II with constraint domination principle (NSGA-II-CDP) to obtain the Pareto-optimal set. Then, a maximum gradient principle of investment revenue is proposed to select the optimal planning strategy from the derived Pareto-optimal solution set, when taking the investment return ratio as primary consideration. The effectiveness of the developed methodology is justified by applying it to a case TN with 25 nodes.

This paper brings the following key contributions:

(a) It introduces a method for calculating the TDfC of EVs in TN and analyzes the probabilistic characteristic of the TDfC.
(b) It originally develops a chance-constraint multiobjective optimization model to minimize both the average TDfC of EVs and the investment of EVCN construction by optimizing the locations of EVCSs.
(c) It customizes the NSGA-II-CDP to solve the developed EVCN planning model, by designing a special coding scheme, a crossover operator, and a mutation operator.
(d) It proposed a maximum gradient principle of investment revenue, which can be used to select the optimal EVCN planning strategies from the Pareto-optimal solution set, when taking the investment return ratio as primary consideration.

This paper is organized as follows. As a basis for modeling, the details of TDfC calculation for EVs are discussed in

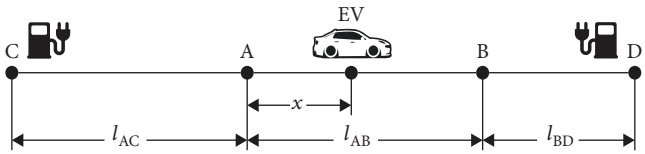

FIGURE 1: TDfC of EVs.

Section 2. Then, a multiobjective EVCN planning model considering chance constraints on EV's TDfC is developed in Section 3. Section 4 customizes the NSGA-II-CDP to solve the developed EVCN planning model. To validate the developed model and solution method, a case study is presented in Section 5. At last, the conclusion of the paper is summarized in Section 6.

2. TDfC Calculation for EVs

Compared to PMM, the FCLM could consider the charging demands of EVs in both scenarios of driving and stopping in the TN, as illustrated in Section 1.2. Therefore, a method to calculate random TDfC of EVs based on counting the EV flows in the TN by the FCLM is developed in this paper. In addition, the Floyd algorithm, also known as the interpolation method, is an algorithm that uses the idea of dynamic programing to find the shortest path between multiple source points in a given weighted graph with positive or negative edge weights [31]. The set of the shortest path in TN is derived by the Floyd algorithm in this paper.

Currently, with the rapid development of smart terminals and wireless communication technology, navigation software, such as Google Maps, has been widely used. Therefore, it can be assumed that EV owners follow the shortest path planned by the navigation software while driving [32]. According to the realistic origin and destination flow structure, which is provided by a simple gravity spatial interaction model [19], the EV flow f_q for the shortest path q, can be defined as follows:

$$f_q = \frac{W_{S,q} W_{E,q}}{1.5 d_q} q \in \Omega_q, \tag{1}$$

where $W_{S,q}$, and $W_{E,q}$ are the weights of origin and destination of the shortest path q, respectively; Ω_q is a set of the shortest path in TN derived by the Floyd algorithm; d_q is the length of the shortest path q, which can be calculated by the set and length that the path q passes.

When an EV needs to be charged at any point in TN, the owners will drive to the closest EVCS according to the navigation software. The scenario is shown below.

Figure 1 is an example to present how to calculate TDfC of EVs. In Figure 1, both A and B are traffic nodes in TN and do not have EVCSs; AB is a road in TN with a length of l_{AB}; the closest EVCS to Node A is located at Node C in TN, AC is the shortest path from A to C with a length of l_{AC}; similarly, the closest EVCS to Node B is located at Node D in TN, BD is the shortest path from B to D with a length of l_{BD}. Both AC and BD are elements in Ω_q. An EV is assumed to be located between A and B with a distance of x to A. There will be two optional charging strategies for the EV: (1) driving through Node A to the EVCS at Node C with a TDfC of $l_{AC} + x$; (2) driving through Node B to the EVCS at Node D with a TDfC of $l_{BD} + l_{AB} - x$. Assuming that the EV owner will drive to the closest EVCS for charging, the TDfC of the EV $T(x)$ illustrated in Figure 1 can be calculated as follows:

$$T(x) = \min[l_{AC} + x, l_{AB} + l_{BD} - x] 0 \le x \le l_{AB}. \tag{2}$$

In addition, if there is an EVCS in Node A or B, l_{AC} or l_{BD} equals to 0 in Equation (2), respectively. Equation (2) demonstrates that EVs' TDfC is related to the multiple variables, e.g., the topology of TN, the deployment of EVCSs in TN, and the locations of EVs on the road.

3. EVCN Planning Model

Based on the EV flow on each shortest path in the TN, a multiobjective EVCN planning model is developed here to optimize locations of a fixed number of EVCSs for achieving two objectives: (1) to minimize average TDfC of EVs, and (2) to minimize investment of the EVCN construction. In the developed EVCN planning model, constraint on the TDfC of EVs is presented as a chance constraint according to the random characteristics of EVs' TDfC.

3.1. Objectives. The developed EVCN planning model contains two objectives, which is to minimize both the average TDfC of all EVs in TN and the overall investments of the EVCN.

For an EVCN, its main function is to provide convenient charging services for EVs. In TN, EVs could drive on any road and stay at any location on different roads. It implies that the location of any EV is a random variable. When charging is required, EV owners would rush into the EVCS with the shortest distance or the least driving time. Therefore, Objective 1 of the developed EVCN planning model is to minimize the average TDfC of all EVs in TN, as shown by:

$$\min T_{ave} = \frac{\sum_{i \in \Omega_R} f_i T_{av,i}}{\sum_{i \in \Omega_R} f_i}, \tag{3}$$

where T_{ave} is a weighted average from the average TDfC of EVs on each road in TN and represents the average TDfC of all EVs in TN, the EV flows on the roads are the weighting factors; the road set in TN is represented by Ω_R; f_i is the EV flows on the i^{th} road and summed from EV flows of the passing shortest path in the shortest paths set Ω_q; $T_{av,i}$ is the average TDfC of EVs on the i^{th} road, and can be given by:

$$T_{\mathrm{av},i} = \int_0^{l_{\mathrm{d},i}} \frac{T_i(x)}{l_{\mathrm{d},i}} dx, \tag{4}$$

where $l_{\mathrm{d},i}$ is the length of the i^{th} road; x is the distance of the EV to be charged from the vertex of the i^{th} road, it is assumed to follow a uniform distribution at the range of $[0, l_{\mathrm{d},i}]$ as a random variable; $T_i(x)$ is defined in Equation (2), representing the TDfC of the EV on the i^{th} road.

Objective 2 of the developed EVCN planning model is to minimize the overall investments of the EVCNs, as given by:

$$\min C_{\mathrm{total}} = \sum_{j=1}^{N} C_{\mathrm{con},j} y_j, \tag{5}$$

where C_{total} is the overall investments of EVCNs; $C_{\mathrm{con},j}$ is the investment of deploying an EVCS at candidate site j, including land occupation cost, equipment cost, operation-maintenance cost, and extra energy losses cost in PDS resulting from supplying power for the EVCS; y_j is a 0–1 binary optimization variable in the developed EVCN planning model: $y_j = 1$, if deploying the EVCS at candidate site j; $y_j = 0$, otherwise.

3.2. Constraints. The developed EVCN planning model considers two constraints, i.e., chance constraint on TDfc and constraint on the number of planned EVCS.

Currently, the range of most EVs is still less than that of traditional fossil fuel vehicles. Therefore, EVs' TDfC is expected to be less than a given threshold in the EVCN planning model. However, EVs' TDfC is random. If we manually set distances less than the given threshold, the optimization would generate unreasonable results. Therefore, the constraint on EVs' TDfC is defined using a chance constraint, as given by:

$$P_{\mathrm{r}}\{\varphi_{\mathrm{d-char}} \le T_{\mathrm{cha-lim}}\} = \frac{\sum_{i\in\Omega_{\mathrm{R}}} f_i p_i}{\sum_{i\in\Omega_{\mathrm{R}}} f_i} \ge \beta, \tag{6}$$

where $P_{\mathrm{r}}\{\cdot\}$ is the probability of the occurrence of the event in the brace; $\varphi_{d\text{-char}}$ represents the TDfC of EVs in TN as a random variable; $T_{\mathrm{cha-lim}}$ is the given range threshold. The lower the $T_{\mathrm{cha-lim}}$, the better the charging convenience provided by the EVCN; β is a confidence level of satisfying the constraint on the TDfC of EVs, the higher the β, the better the charging convenience provided by the EVCN. p_i is the probability that the TDfC of EVs on the i^{th} road is less than the given range threshold, which can be given by:

$$p_i = \int_0^{l_{\mathrm{d},i}} \frac{g_i(x)}{l_{\mathrm{d},i}} dx, \tag{7}$$

where $g_i(x)$ is an auxiliary function to judge whether the TDfC of EV (which is x apart from the vertex of the i^{th} road) is less than the given range threshold, which has two values: 0 or 1, as shown:

$$g_i(x) = \begin{cases} 1, & T_i(x) \le T_{\mathrm{cha-lim}} \\ 0, & T_i(x) \ge T_{\mathrm{cha-lim}} \end{cases} \quad 0 \le x \le l_{\mathrm{d},i}. \tag{8}$$

In the developed EVCN planning model, planners predetermine the number of EVCSs and their candidate sites based on the boundary conditions, e.g., estimated investments, municipal planning, EV penetration rate, and so on. Hence, there is an additional constraint on the number of EVCS constructed in the model, as given by:

$$M = \sum_{j=1}^{N} y_j, \tag{9}$$

where M is the number of EVCSs to be constructed.

4. Solution Method

The developed EVCN planning model is a chance-constraint binary programing problem with two optimization objectives. There is a lack of clear analytical expressions among optimization objectives, constraints, and control variables. Therefore, it is difficult to adopt traditional mathematical solvers, e.g., a general algebraic modeling system to solve the developed EVCN planning model.

To achieve multiobjective optimization, it requires coordinating relationships among multiple objectives to obtain a solution set [33]. The constrained multiobjective evolutionary algorithms (CMOEAs) can coordinate multiple objectives in the optimization, thus giving the solution set of the multiobjective optimization [34–37]. NSGA-II-CDP is a famous CMOEA, which is customized and then utilized to solve the developed EVCN planning model in this paper.

4.1. Solving Framework. Figure 2 presents a flowchart for solving the EVCN planning model developed by the custom NSGA-II-CDP.

In Figure 2, N_{pop} is the population size, i.e., the number of chromosomes in the population; g is an index of evolutional generation; $T_{\mathrm{ave},k}$ represents an average TDfC of all EVs to the closest EVCS when the EVCN is constructed according to the deployment strategy given by the k^{th} chromosome; $C_{\mathrm{total},k}$ is an overall investment of the EVCN, and $P_{\mathrm{ev},k}$ represents a probability that the TDfC of EVs is less than the given threshold; $G_{\max}$ is a predetermined maximum evolutionary generation. The customized NSGA-II-CDP stops when the evolution reaches the maximum generation.

4.2. Detailed Solution Procedure. The detailed solution using the custom NSGA-II-CDP for the developed EVCN planning model is as follows:

4.2.1. Calculations of Parameters in TN. First, the shortest path set Ω_q of the TN is derived by the Floyd algorithm according to the TN topology. Then, EV flows f_q ($q \in \Omega_q$) on each shortest path are calculated according to Equation (1). At last, EV flows f_i ($i \in \Omega_R$) on each road are calculated by summing the EV flows.

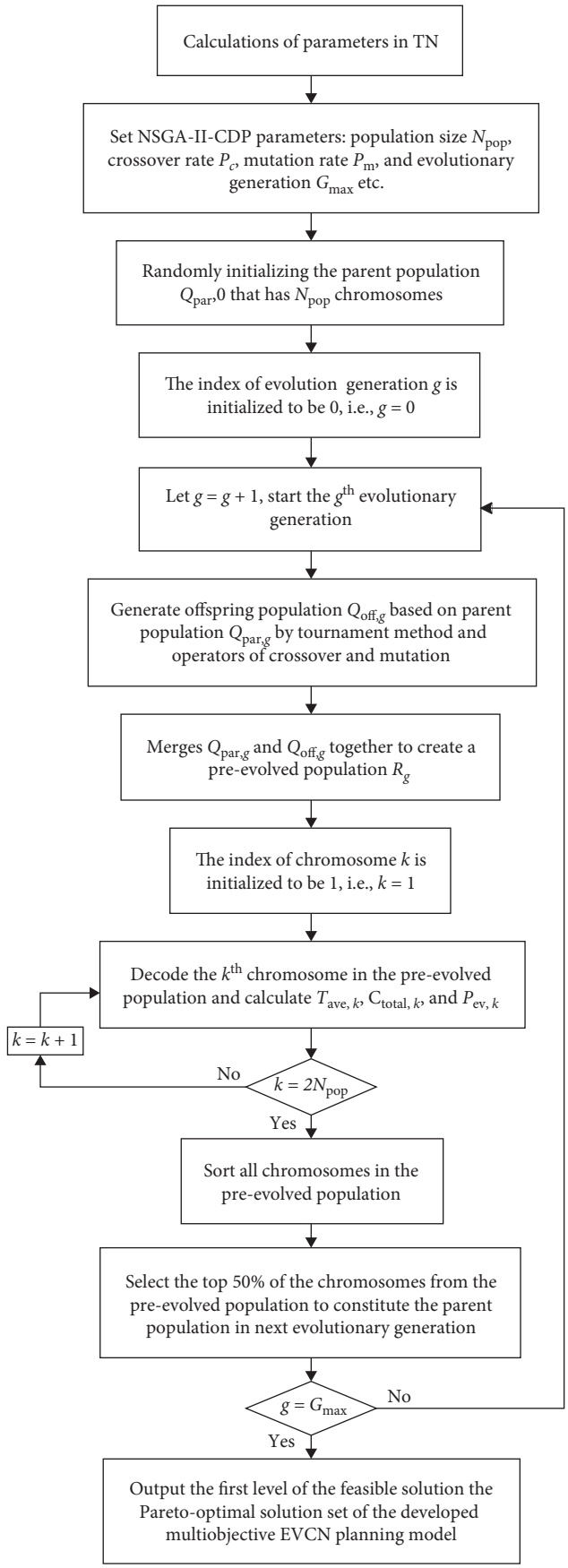

Figure 2: The flowchart for solving the EVCN planning model developed by the custom NSGA-II-CDP.

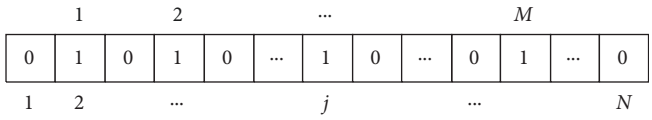

Figure 3: Encoding scheme of the chromosome.

4.2.2. Chromosome Coding and Population Initialization. The developed EVCN planning model is a binary programing problem, we use a binary-coded approach for encoding and getting chromosomes, i.e., the solution is represented by a binary code string with the length of N, as illustrated in Figure 3.

The binary code string illustrated in Figure 3 represents a solution of the developed EVCN planning model. In Figure 3, the value at the j^{th} coding point represents whether deploying an EVCS at the j^{th} candidate site: if the value is equals to "1", an EVCS is deployed at the j^{th} candidate site; otherwise, there is no deployment plan. To match the constraint on the number of EVCSs given by Equation (9), there should be only M coding points having the value of "1" in Figure 3.

In this paper, the parent population in the g^{th} evolutionary generation is entitled as $Q_{\text{par},g}$. When initializing the parent population, the index of evolutional generation g is set to be 0. Therefore, the initial parent population can be entitled $Q_{\text{par},\,0}$ and generated as the following steps:

(a) Values of all coding points of each chromosome are set to be "0";

(b) For each chromosome, M coding points are randomly selected and their values are changed from "0" to "1".

4.2.3. Create a Pre-Evolved Population. Two chromosomes from the parent population $Q_{\text{par},g}$ are randomly selected, the better one is copied to the offspring population $Q_{\text{off},g}$. This process is repeated until the number of chromosomes in $Q_{\text{off},g}$ reaches N_{pop}. The basis for selecting better chromosomes can be found in 4.2.4.

$Q_{\text{off},\,g}$ is updated by applying crossover and mutation operations to chromosomes in $Q_{\text{off},g}$, respectively, at pretermitted probabilities. The operators of crossover and mutation are detailed as follows. Then, $Q_{\text{par},g}$ and $Q_{\text{off},g}$ are merged to create a pre-evolved population R_g ($R_g = Q_{\text{par},g} \cup Q_{\text{off},g}$) which has $2N_{\text{pop}}$ number of chromosomes.

(1) *Crossover operator*. To ensure that the postcrossover chromosome satisfies the constraint on the number of EVCSs as given by Equation (9), the conventional crossover operator is improved as detailed shown in Figure 4.

The improved crossover operator has three steps, detailed as follows:

Step 1: two chromosomes are selected randomly from the population as the precrossed chromosomes.

Step 2: a coding point N_{cro} ($1 < N_{\text{cro}} < N$) is randomly selected as the precrossed point; if these two chromosomes have the same coding point number equal to "1" behind N_{cro}, the coding point N_{cro} is considered a feasible crossed point N_{ave}; otherwise, this process is repeated until the feasible crossed point N_{ave} that satisfies the above demand is found.

Step 3: the coding string is exchanged behind N_{ave} at a crossover probability of P_{c}.

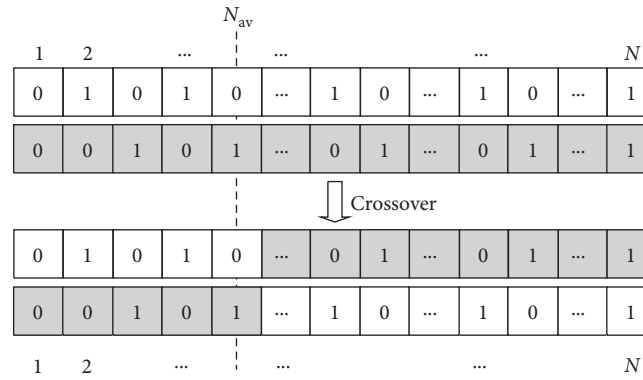

Figure 4: The improved cross-operator.

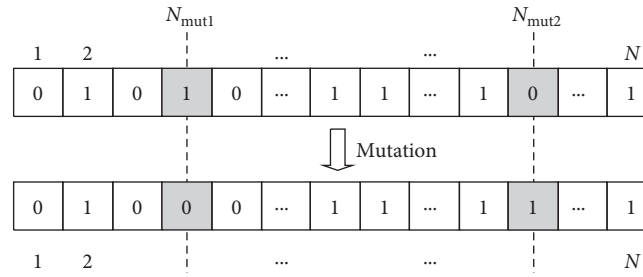

Figure 5: The developed two-point mutation operator.

(2) *Mutation operator*. To ensure the postmutation chromosome satisfies the constraint on the number of EVCSs as given by Equation (9), a two-point mutation operator is developed by improving the conventional single-point mutation operator, as illustrated in Figure 5.

The developed two-point mutation operator has three steps, detailed as follows:

Step 1: a chromosome is randomly selected from the population as the premutated chromosome.

Step 2: two different coding points N_{mut1} and N_{mut2} ($1 \le N_{\text{mut1}} \le N$, $1 \le N_{\text{mut2}} \le N$) as the premutated coding points are randomly selected, the values of the coding points N_{mut1} and N_{mut2} should be different.

Step 3: the values of the coding points N_{mut1} and N_{mut2} are changed simultaneously at a mutation probability of P_{m}.

4.2.4. Elitism Selection Strategy for the Pre-Evolved Population. All chromosomes are decoded in the pre-evolved population R_g to derive the EVCS deployment strategy represented by each chromosome in the pre-evolved population. $2N_{\text{pop}}$ chromosomes in the pre-evolved population correspond to their own solutions of the developed EVCN planning model. Both

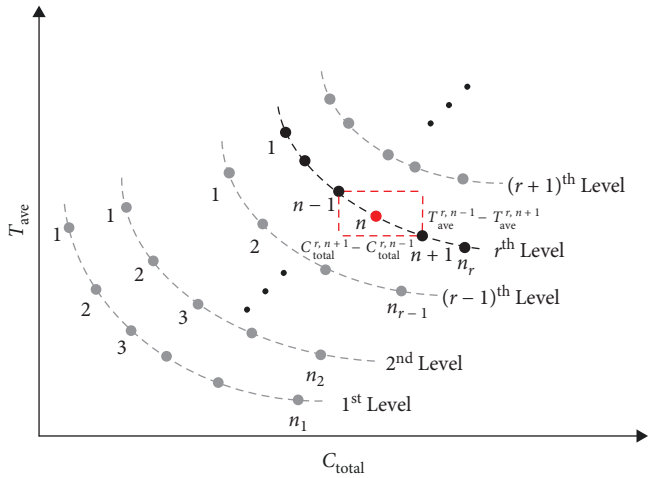

FIGURE 6: Nondominated sorting results for all feasible solutions.

the parent and offspring populations satisfy the constraint on the number of EVCS, since the number of EVCS is set in advance and the improved crossover and mutation operators are designed for evolution. Thus, the pre-evolved population can be divided into two categories on whether the solution can meet the chance constraint on the TDfC of EVs. The solutions that satisfy the constraint are feasible, and the unsatisfied solutions are unfeasible. All chromosomes in the pre-evolved population are reordered according to the following rules [35, 36].

(a) Any feasible solution should be better than an unfeasible solution.

(b) According to the Pareto-dominance principle, nondominated sorting is executed for all feasible solutions, thus all feasible solutions are divided into several levels, as illustrated in Figure 6. If feasible solutions are on the different levels, the solutions at a more forward level are better than the others.

(c) If solutions are on the same level, they can be evaluated by an assigned fitness, i.e., the solution with a greater assigned fitness is better. In order to calculate the assigned fitness, all feasible solutions on each level are first arranged according to the value of C_{total}, as illustrated in Figure 6. Then, as introduced in [36], the assigned fitness of all feasible solutions on each level is determined according to Equation (10).

$$F_{r,n} = \begin{cases} \left(C_{total}^{r,n+1} - C_{total}^{r,n-1}\right) + \left(T_{ave}^{r,n-1} - T_{ave}^{r,n+1}\right) & 1 < n < n_r \\ K & n = 1, n_r \end{cases}, \tag{10}$$

where n is the index of the solutions on the same level; r is the index of the level; $F_{r,n}$ is the assigned fitness of the n^{th} solution on the r^{th} level; n_r is the number of solutions on the r^{th} level; $C_{total}^{r,n}$ and $T_{ave}^{r,n}$ are, respectively, the C_{total} and T_{ave} of the n^{th} solution on the r^{th} level; K is a predetermined maximal number.

(d) For an unfeasible solution, the degree of violating against the chance constraint is entitled as C_V, which is given by Equation (11).

$$C_V = \left| \frac{p_{ev}}{\beta} - 1 \right|. \tag{11}$$

The value of C_V determines the order of unfeasible solutions, i.e., the less the violating degree, the higher the ranking in the order.

After reordering $2N_{pop}$ chromosomes according to the principles described above, the top 50% of the chromosomes from the pre-evolved population are selected as the elitisms to constitute the parent population in the next evolutionary generation.

(e) When the evolution reaches the maximum evolutionary generation, the chromosomes in the first level of the feasible solution are outputted as the Pareto-optimal solution set of the developed multiobjective EVCN planning model, thus ending the customized NSGA-II-CDP process.

4.3. The Optimal Deployment Strategy. The set of Pareto-optimal solutions derived by the custom NSGA-II-CDP contains multiple nondominated solutions. This leads to the problem that these nondominated solutions cannot be compared due to the conflict between two objectives of the developed EVCN planning model, that is, these two objectives cannot reach the optimum at the same time.

The choice of the optimal deployment strategy depends on the decision maker's subjective desires, which can be considered in three cases: (a) if the investment capital is very limited, the Pareto-optimal solution with the minimum C_{total} is chosen; (b) if the goal is to minimize the average TDfC of EVs regardless of the cost, the optimal solution with the minimum T_{ave} is chosen; (c) if these two objectives need to be taken into account at the same time, that is, taking the investment return ratio as primary consideration, a maximum gradient principle of investment revenue is proposed to select the optimal solution from the Pareto-optimal solution set.

The detailed steps of the maximum gradient principle of investment revenue are described below.

(a) All solutions in the Pareto-optimal solution set are sorted according to C_{total} of the solution, from smallest to largest, thus the first solution is the one with the least investment.

(b) Excluding the first solution in the Pareto-optimal solution set, investment revenue gradients of the other solutions are calculated by Equation (12).

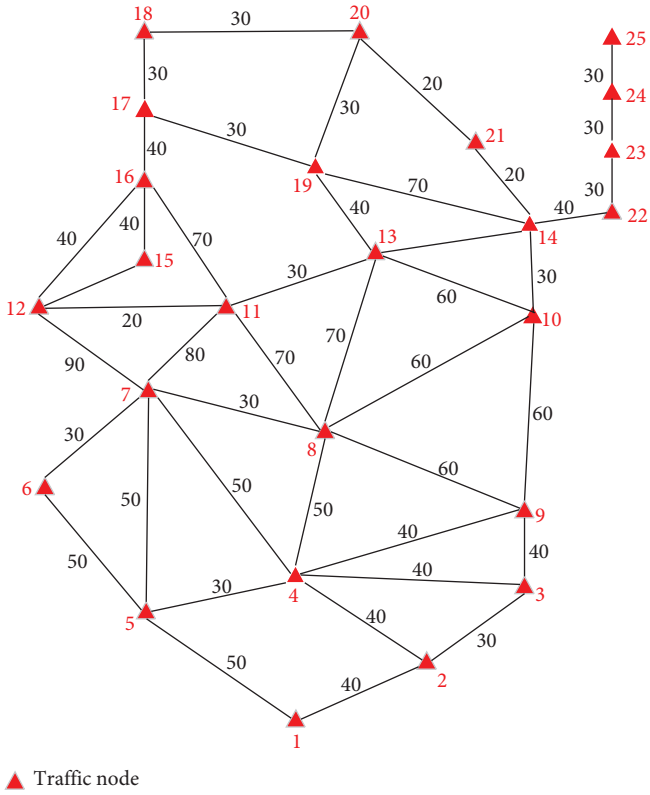

Figure 7: The topology of the 25-node TN.

Table 1: Weight coefficients of nodes in the 25-node TN.

Node	Weight	Node	Weight	Node	Weight
1	0.54	10	0.54	19	0.80
2	0.80	11	0.05	20	0.27
3	0.27	12	0.54	21	0.27
4	0.27	13	0.05	22	0.54
5	0.27	14	0.54	23	0.05
6	0.07	15	0.27	24	1.34
7	0.05	16	0.27	25	0.05
8	0.54	17	0.27		
9	0.27	18	1.07		

Table 2: Construction costs for EVCS at each candidate site.

Node	Cost /$10^6 \cdot$¥	Node	Cost /$10^6 \cdot$¥	Node	Cost /$10^6 \cdot$¥
1	5	10	10	19	10
2	5	11	8.6	20	24
3	5	12	8.6	21	6
4	9	13	9	22	10
5	23	14	24	23	6
6	4.6	15	8.6	24	6
7	8.6	16	22.6	25	6
8	24	17	5		
9	10	18	5		

$$E_h = \frac{T_{\text{ave},1} - T_{\text{ave},h}}{C_{\text{total},h} - C_{\text{total},1}} \quad 1 < h \le H, \tag{12}$$

where h is the index of the solution in the Pareto-optimal solution set; H is the number of solutions in the Pareto-optimal solution set; $T_{\text{ave},h}$ and $C_{\text{total},h}$ are, respectively, the average TDfC of all EVs in TN and the overall investments of the EVCN corresponding to the h^{th} solution; E_h is the gradient of investment revenue of the h^{th} solution.

(c) The solution with the maximum gradient of investment revenue in the Pareto-optimal solution set is taken as the optimal deployment strategy of the EVCN.

5. Case Study

The developed EVCN planning model and NSGA-II-CDP-based solving method are validated by a case study based on a 25-node TN.

5.1. Case Detail. The topology of the 25-node TN is shown in Figure 7, which contains 25 nodes and 43 roads. In Figure 7, the red numbers indicate the node numbers, and the black numbers on the lines whose units are kilometers represent the link lengths between the nodes. Each node in the TN is a candidate site for EVCS. The weight of each node is introduced in Table 1 [19], and the construction costs of EVCS at each candidate site are presented in Table 2.

In the case study, each road is supposed to be bidirectional, i.e., the shortest path from the start node to the end node is the same as that from the end node to the start node. Therefore, the shortest path set Ω_q contains 300 shortest paths (i.e., $(25\times(25-1))/2 = 300$). All shortest paths in the TN together with the traffic nodes and roads passing by each shortest path can be determined by the Floyd algorithm. The overall EV flows on all the shortest paths and roads are 0.307 and 0.84, respectively.

The number of planned EVCSs is set to be four in this paper. The driving range of the mainstream EVs at the maximum state-of-charge (SOC) is between 300 and 500 km. Most EV owners would charge their EVs at about 20% SOC. Therefore, the threshold of EVs' TDfC $T_{\text{cha-lim}}$ and the confidence level β are, respectively, set as 80 km and 95%.

5.2. Solution of the Developed EVCN Planning Model by the Customized NSGA-II-CDP. Before solving the developed EVCN planning model by the customized NSGA-II-CDP, the relevant parameters are set as follows: the population size N_{pop} is 100; the maximum evolutionary generation $G_{\max}$ is 150; the crossover probability P_c; and the mutation probability P_m are, respectively, 0.05 and 0.1.

The planning strategies derived in the set of Pareto-optimal solutions are shown in Table 3. All planning strategies have been reordered according to C_{total} of each strategy.

Table 3: The planning results in the set of Pareto-optimal solutions ($\beta = 95\%$ and $M = 4$).

Planning strategy	T_{ave}/km	C_{total} /$10^6 \cdot$¥	p_{ev} (%)	The locations of the EVCSs
1	43.42	25	95.28	3、13、18、23
2	36.72	25.6	96.04	3、11、21、23
3	35.58	29.6	99.81	4、12、21、23
4	35.22	43.6	95.62	4、11、14、17
5	35.18	47.6	95.54	4、11、14、23
6	34.95	48	95.53	4、13、14、23
7	34.08	49	95.06	4、14、19、23

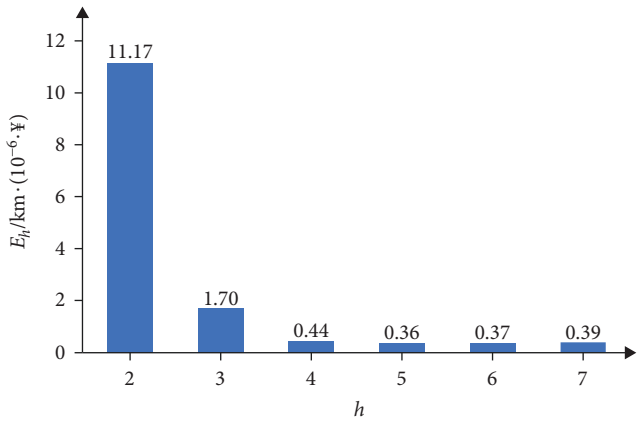

Figure 8: Gradient of investment revenue of all planning strategies except the first one ($\beta = 95\%$ and $M = 4$).

There are seven planning strategies in the set of Pareto-optimal solutions. T_{ave} is longest at 43.42 km and C_{total} is 25×10^6¥ in the first planning strategy. Whereas, in the 7th planning strategy, T_{ave} and C_{total} are, respectively, 34.08 km and 49×10^6¥. Compared to the first planning strategy, T_{ave} in the 7th planning strategy is 21.5% shorter, equivalent to 9.34 km. However, the investments C_{total} increases by 96%, equivalent to 24×10^6¥. A short average TDfC of EVs brings a significant increase in the investment. Therefore, it is necessary to select the optimal strategy from the seven planning strategies based on the maximum marginal revenue principle.

According to the steps described in Section 4.3, the gradients of investment revenue of all planning strategies are calculated except the first one, which are shown in Figure 8.

Figure 8 presents that the 2nd planning strategy has the highest marginal investment revenue, which is 11.17 km/10^6¥. The 2nd planning strategy is therefore selected as the optimal planning strategy of the case study.

For the 2nd planning strategy, the locations of the planned EVCSs are nodes 3, 11, 21, and 23, as illustrated in Figure 9. T_{ave} is 36.72 km, C_{total} is 25.6×10^6¥, and the p_{ev} is 96.04%. Figures 10 and 11 are, respectively, the probability density function (PDF) and the cumulative distribution function (CDF) of random EVs' TDfC corresponding to the 2nd planning strategy. Figures 10 and 11 present that the maximum TDfC of few EVs can exceed 110 km, but 96.04% of EVs have a TDfC less than the 80 km threshold, according to

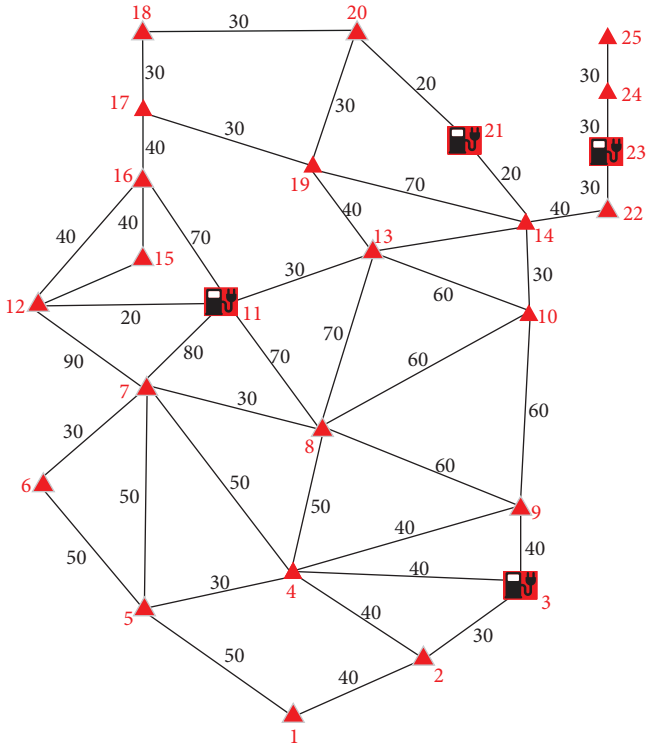

Figure 9: The optimal planning strategy of the case study ($\beta = 95\%$ and $M = 4$).

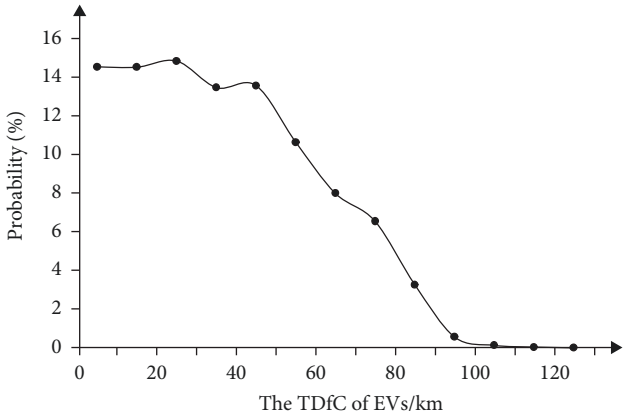

Figure 10: The PDF of the EVs' TDfC corresponding to the optimal planning strategy ($\beta = 95\%$ and $M = 4$).

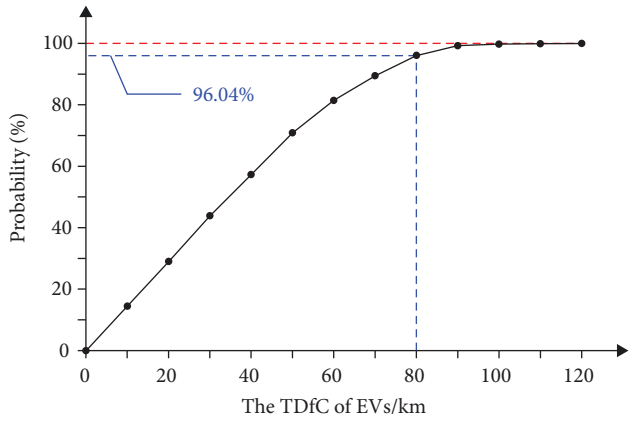

Figure 11: The CDF of the EVs' TDfC corresponding to the optimal planning strategy ($\beta = 95\%$ and $M = 4$).

Table 4: The planning results in the Pareto-optimal solution set ($\beta = 90\%$ and $M = 4$).

Planning strategy	T_{ave}/km	C_{total} /$10^6 \cdot$¥	p_{ev} (%)	The locations of the EVCSs
1	45.14	24.2	90.76	3、6、12、21
2	43.42	25	95.28	3、13、18、23
3	36.72	25.6	96.04	3、11、21、23
4	36.30	26	92.97	4、17、21、23
5	35.58	29.6	99.81	4、12、21、23
6	33.99	44	93.31	4、14、17、23

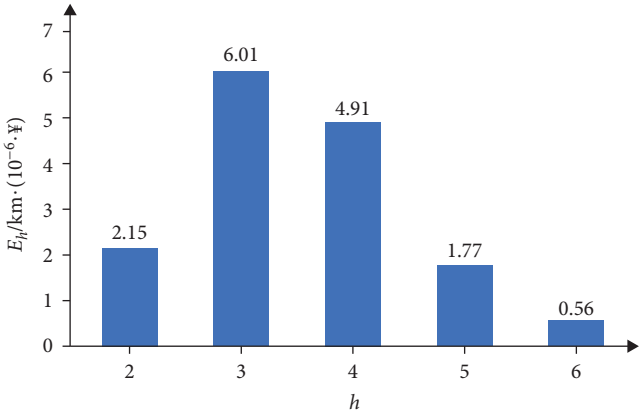

Figure 12: Gradient of investment revenue of all planning strategies except the first one ($\beta = 90\%$ and $M = 4$).

the 2nd planning strategy. This follows the chance constraint on EVs' TDfC given by Equation (6).

5.3. The Impact of Confidence Level on the Planning Results. The confidence level β is an important parameter in the developed EVCN planning model, which is predetermined by the planners. When the confidence level β decreases from 95% to 90%, the derived planning strategies in the Pareto-optimal solution set change accordingly, as illustrated in Table 4. The gradients of investment revenue of the planning strategies 2, 3, 4, 5, and 6 given in the Table 4 are calculated and presented in Figure 12.

Table 5: The optimal planning strategies corresponding to different numbers of planned EVCSs ($\beta = 95\%$).

M	T_{ave}/km	C_{total}/ $10^6 \cdot$¥	The locations of the EVCSs
4	36.72	25.6	3、11、21、23
5	35.48	30.2	3、6、11、21、23
6	30.3	35.2	3、6、11、17、21、23
7	28.68	40.2	2、3、6、11、17、21、23
8	27.54	45.2	2、3、6、11、17、18、21、23
9	22.22	59.2	2、3、7、10、11、17、18、21、23
10	24.83	59.2	1、2、3、4、6、11、17、18、21、23

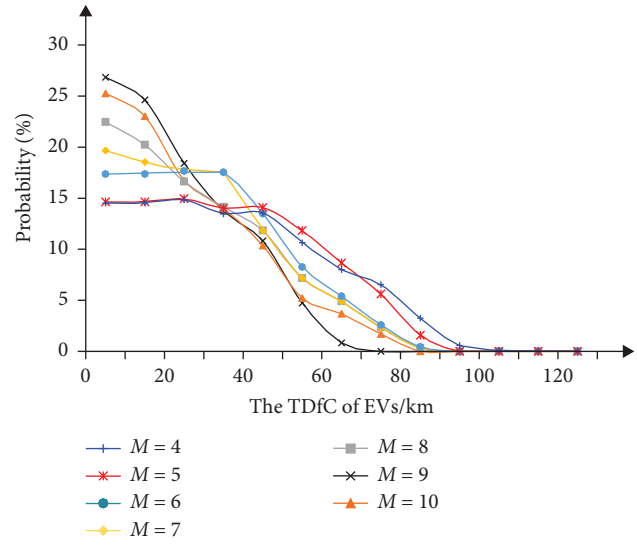

Figure 13: The PDF of the EVs' TDfC corresponding to different numbers of planned EVCSs.

Tables 3 and 4 show that a different Pareto-optimal solution set appears when reducing the confidence level β from 95% to 90%. The number of Pareto-optimal solutions reduces from 7 to 6 resulting from reducing the 5% confidence level. For this case, the minimum and maximum values of T_{ave} are 33.99 and 45.14 km, respectively, and the corresponding C_{total} are 44×10^6¥ and 24.2×10^6¥.

Figure 12 presents that the 3rd planning strategy in the Pareto-optimal solution set is an optimal one, because it has the maximum value of E_h, which is 6.01 km/10^6¥. Further observation shows that the 3rd planning strategy in Table 4 is the same as the 2nd one in Table 3. When the confidence level decreases from 95% to 90%, the optimal planning strategy does not change, despite a different Pareto-optimal solution. However, the comparison between Figures 8 and 12 shows that the advantage of the optimal solution over other solutions decreases with the decrease in confidence level.

5.4. The Planning Results in Different Numbers of EVCSs. In previous cases, the number of planned EVCSs is set to 4. As an important boundary condition, the number of planned EVCSs may delivers a significant impact on the planning results. Table 5 shows the optimal planning strategies corresponding to the different numbers of planned EVCSs.

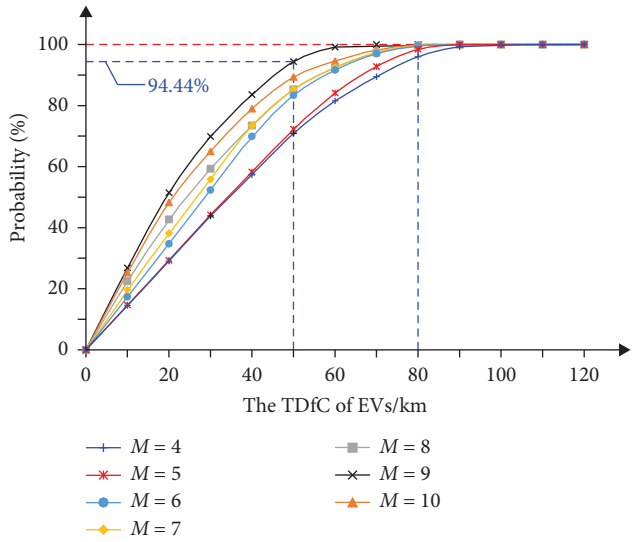

FIGURE 14: The CDF of the EVs' TDfC corresponding to different numbers of planned EVCSs.

Table 5 shows that T_{ave} would decrease and C_{total} would increase consistently with the increasing number of planned EVCSs. When the number of planned EVCSs increases from 9 to 10, C_{total} remains unchanged, equals 59.2×10^6 ¥, however, T_{ave} increases from 22.22 to 24.83 km. It shows that a greater number of the planned EVCSs is not always better. Therefore, planners should take a comprehensive consideration of the number of the planned EVCSs in the developed EVCN.

Figures 13 and 14 present the PDF and the CDF of the EVs' TDfC in the different numbers of planned EVCSs, respectively. These two figures demonstrate that the different number of planned EVCSs brings different probabilistic characteristics of the EVs' TDfC. The greater the number of planned EVCSs, the higher the probability that the TDfC of the EVs is less than the set threshold. When the number of planned EVCSs is more than 5, the p_{ev} approaches 100%. When the number of planned EVCSs increases to 9, most of the EVs' TDfC is between 0 and 50 km with a probability of 94.44%.

6. Conclusion

To improve the charging convenience of EVs, this paper developed a chance-constraint multiobjective EVCN planning model. With a fixed number of planned EVCSs, the developed EVCN planning model desires to minimize the average TDfC of all EVs in the TN and the investment costs of EVCN by selecting locations of the EVCSs from candidate sites. NSGA-II-CDP is customized and utilized to solve the developed EVCN planning model, thus deriving the Pareto-optimal solution set which contains several planning strategies. In addition, when taking the investment return ratio as primary consideration, a maximum gradient principle of investment revenue is proposed to select the optimal planning strategy from the derived Pareto-optimal solution set, i.e., to determine the optimal deployment strategy of the planned EVCSs.

In this paper, EV flows on each road in the developed EVCN planning model are calculated by the FCLM. In practice, these can also be determined according to the measured traffic data to ensure that the planning strategy obtained through the developed methodology is more suitable for the actual demand.

Abbreviations

EVCSs:	Electric vehicle charging stations
EVs:	Electric vehicles
EVCN:	Electric vehicle charging network
TN:	Traffic network
TDfC:	Travel distance for charging
NSGA-II-CDP:	Nondominated sorting senetic Algorithm II with the constraint domination principle
PDS:	Power distribution system
FCLM:	Flow-capturing location model
FRLM:	Flow-refueling location model
GA:	Genetic algorithm
PMM:	P-median model
SCM:	Set covering model
MCLM:	Maximal covering location model
GAMS:	General algebraic modeling system
CMOEAs:	Constrained multiobjective evolutionary algorithms
PDF:	Probability density function
CDF:	Cumulative distribution function.

Data Availability

The data used to support the findings of this study are available from the corresponding author upon request.

Conflicts of Interest

The authors declare that they have no conflicts of interest.

Acknowledgments

This work was supported in part by the National Natural Science Foundation of China (52377104), the State-Sponsored Visiting Scholar Program of China Scholarship Council (202108320239), the Natural Science Foundation of the Jiangsu Higher Education Institutions of China (22KJA470006 and 20KJA470002), and the Natural Science Foundation of Jiangsu Province (BK20210837).

References

[1] J. Jing, Y. Liu, J. Wu, W. Huang, and B. Zuo, "Research on power management and allowed propulsion control in pure electric vehicle," *Energy Reports*, vol. 8, no. Supplement 1, pp. 178–187, 2022.

[2] Q. Zhao, Z. Wei, H. Liu, Y. Han, and J. Wang, "Optimal semi-dynamic traffic and power flow assignment of coupled transportation and power distribution systems for electric vehicles," *IET Electrical Systems in Transportation*, vol. 13, no. 1, Article ID e12064, 2023.

[3] H. Zhang, Z. Hu, Z. Xu, and Y. Song, "An integrated planning framework for different types of PEV charging facilities in Urban area," *IEEE Transactions on Smart Grid*, vol. 7, no. 5, pp. 2273–2284, 2016.

[4] G. Napoli, A. Polimeni, S. Micari, L. Andaloro, and V. Antonucci, "Optimal allocation of electric vehicle charging stations in a highway network: Part 1. methodology and test application," *Journal of Energy Storage*, vol. 27, Article ID 101102, 2020.

[5] G. Napoli, A. Polimeni, S. Micari, G. Dispenza, and V. Antonucci, "Optimal allocation of electric vehicle charging stations in a highway network: Part 2. the Italian case study," *Journal of Energy Storage*, vol. 26, Article ID 101015, 2019.

[6] S. Singh, R. K. Saket, and B. Khan, "A comprehensive state-of-the-art review on reliability assessment and charging methodologies of grid-integrated electric vehicles," *IET Electrical Systems in Transportation*, vol. 13, no. 1, Article ID e12073, 2023.

[7] R. S. Gupta, A. Tyagi, and S. Anand, "Optimal allocation of electric vehicles charging infrastructure, policies and future trends," *Journal of Energy Storage*, vol. 43, Article ID 103291, 2021.

[8] R. C. Green II, L. Wang, and M. Alam, "The impact of plug-in hybrid electric vehicles on distribution networks: a review and outlook," *Renewable and Sustainable Energy Reviews*, vol. 15, no. 1, pp. 544–553, 2011.

[9] R. S. Gupta, A. Tyagi, and S. Anand, "Optimal planning of EV charging infrastructure in distribution system," in *Signals, Machines and Automation*, A. Rani, B. Kumar, V. Shrivastava, and R. C. Bansal, Eds., vol. 1023 of *SIGMA 2022. Lecture Notes in Electrical Engineering*, pp. 657–667, Springer, Singapore, 2023.

[10] E. Hadian, H. Akbari, M. Farzinfar, and S. Saeed, "Optimal allocation of electric vehicle charging stations with adopted smart charging/discharging schedule," *IEEE Access*, vol. 8, pp. 196908–196919, 2020.

[11] A. K. Venkitaraman and V. S. R. Kosuru, "Electric vehicle charging network optimization using multi-variable linear programming and bayesian principles," in *2022 Third International Conference on Smart Technologies in Computing, Electrical and Electronics (ICSTCEE)*, pp. 1–5, IEEE, Bengaluru, India, December 2022.

[12] F. Alfaverh, M. Denaï, and Y. Sun, "Electrical vehicle grid integration for demand response in distribution networks using reinforcement learning," *IET Electrical Systems in Transportation*, vol. 11, no. 4, pp. 348–361, 2021.

[13] A. Pal, A. Bhattacharya, and A. K. Chakraborty, "Placement of public fast-charging station and solar distributed generation with battery energy storage in distribution network considering uncertainties and traffic congestion," *Journal of Energy Storage*, vol. 41, Article ID 102939, 2021.

[14] L. He, J. He, L. Zhu, W. Huang, Y. Wang, and H. Yu, "Comprehensive evaluation of electric vehicle charging network under the coupling of traffic network and power grid," *PLOS ONE*, vol. 17, no. 9, Article ID e0275231, 2022.

[15] S. Li, Y. Huang, and S. J. Mason, "A multi-period optimization model for the deployment of public electric vehicle charging stations on network," *Transportation Research Part C: Emerging Technologies*, vol. 65, pp. 128–143, 2016.

[16] Y. Honma and M. Kuby, "Node-based vs. path-based location models for urban hydrogen refueling stations: comparing convenience and coverage abilities," *International Journal of Hydrogen Energy*, vol. 44, no. 29, pp. 15246–15261, 2019.

[17] D. Mao, J. Tan, and J. Wang, "Location planning of PEV fast charging station: an integrated approach under traffic and power grid requirements," *IEEE Transactions on Intelligent Transportation Systems*, vol. 22, no. 1, pp. 483–492, 2021.

[18] A. Pal, A. Bhattacharya, and A. K. Chakraborty, "Planning of EV charging station with distribution network expansion considering traffic congestion and uncertainties," *IEEE Transactions on Industry Applications*, vol. 59, no. 3, pp. 3810–3825, 2023.

[19] M. J. Hodgson, "A flow-capturing location–allocation model," *Geographical Analysis*, vol. 22, no. 3, pp. 270–279, 1990.

[20] M. Kuby and S. Lim, "The flow-refueling location problem for alternative-fuel vehicles," *SocioEconomic Planning Sciences*, vol. 39, no. 2, pp. 125–145, 2005.

[21] I. Capar, M. Kuby, V. J. Leon, and Y.-J. Tsai, "An arc cover–path-cover formulation and strategic analysis of alternative-fuel station locations," *European Journal of Operational Research*, vol. 227, no. 1, pp. 142–151, 2013.

[22] A. A. Kadri, R. Perrouault, M. K. Boujelben, and C. Gicquel, "A multi-stage stochastic integer programming approach for locating electric vehicle charging stations," *Computers & Operations Research*, vol. 117, Article ID 104888, 2020.

[23] C. Lee and J. Han, "Benders-and-price approach for electric vehicle charging station location problem under probabilistic travel range," *Transportation Research Part B: Methodological*, vol. 106, pp. 130–152, 2017.

[24] S. L. Hakimi, "Optimum locations of switching centers and the absolute centers and medians of a graph," *Operations Research*, vol. 12, no. 3, pp. 450–459, 1964.

[25] S. L. Hakimi, "p-Median theorems for competitive locations," *Annals of Operations Research*, vol. 6, no. 4, pp. 75–98, 1986.

[26] R. Roth, "Computer solutions to minimum-cover problems," *Operations Research*, vol. 17, no. 3, pp. 455–465, 1969.

[27] C. Toregas, R. Swain, C. ReVelle, and L. Bergman, "The location of emergency service facilities," *Operations Research*, vol. 19, no. 6, pp. 1363–1373, 1971.

[28] R. Church and C. ReVelle, "The maximal covering location problem," *Papers of the Regional Science Association*, vol. 32, pp. 101–118, 1974.

[29] F. Colombo, R. Cordone, and G. Lulli, "The multimode covering location problem," *Computers & Operations Research*, vol. 67, pp. 25–33, 2016.

[30] S. Y. He, Y.-H. Kuo, and D. Wu, "Incorporating institutional and spatial factors in the selection of the optimal locations of public electric vehicle charging facilities: a case study of Beijing, China," *Transportation Research Part C: Emerging Technologies*, vol. 67, pp. 131–148, 2016.

[31] A. Pradhan and G. K. Mahinthakumar, "Finding all-pairs shortest path for a large-scale transportation network using parallel Floyd–Warshall and parallel Dijkstra algorithms," *Journal of Computing in Civil Engineering*, vol. 27, no. 3, pp. 263–273, 2013.

[32] L. Luo, W. Gu, Z. Wu, and S. Zhou, "Joint planning of distributed generation and electric vehicle charging stations considering real-time charging navigation," *Applied Energy*, vol. 242, pp. 1274–1284, 2019.

[33] N. Srinivas and K. Deb, "Muiltiobjective optimization using nondominated sorting in genetic algorithms," *Evolutionary Computation*, vol. 2, no. 3, pp. 221–248, 1994.

[34] Z.-Z. Liu and Y. Wang, "Handling constrained multiobjective optimization problems with constraints in both the decision and objective spaces," *IEEE Transactions on Evolutionary Computation*, vol. 23, no. 5, pp. 870–884, 2019.

[35] H. Lin, Z. Fan, X. Cai et al., "Hybridizing infeasibility driven and constrained-domination principle with MOEA/D for constrained multiobjective evolutionary optimization," in

Technologies and Applications of Artificial Intelligence, S. M. Cheng and M. Y. Day, Eds., vol. 8916 of *TAAI 2014. Lecture Notes in Computer Science*, pp. 249–261, Springer, Cham, 2014.

[36] K. Deb, "An efficient constraint handling method for genetic algorithms," *Computer Methods in Applied Mechanics and Engineering*, vol. 186, no. 2-4, pp. 311–338, 2000.

[37] K. Deb, A. Pratap, S. Agarwal, and T. Meyarivan, "A fast and elitist multiobjective genetic algorithm: NSGA-II," *IEEE Transactions on Evolutionary Computation*, vol. 6, no. 2, pp. 182–197, 2002.